Three-dimensional maps of power quality loss based in the power tensor theory

Mapas tridimensionales de pérdida de la calidad de potencia basados en la teoría tensorial de la potencia

A.J. Ustariz-Farfan[1], E.A. Cano-Plata[2], and H.E. Tacca[3]

***Abstract*— This paper presents the results of a project which was aimed at developing a flexible visualisation tool to be used mainly by power system operators. The project concentrated on a technique for assessing the deterioration of power transfer quality in electrical networks based on the power tensor theory. One of the envisioned tool's essential goals was to aid system operators by providing images of the system with easily identifiable characteristics related to loss or overall deterioration of power quality. The result was a user-friendly, three-dimensional graphic interface. The tool's effectiveness has been illustrated via different scenarios created using the IEEE 13-bus test feeder as an example.**

***Keyworsds*— power quality assessment, power quality map, power quality measurement, tensor analysis**

***Resumen*— Este artículo presenta los resultados de una investigación relacionada con el desarrollo de una herramienta de visualización flexible, para ser usado principalmente por los operadores del sistema eléctrico. La investigación se centró en una técnica para evaluar el deterioro de la calidad de la potencia transmitida en redes eléctricas, basada en la teoría del tensor de potencia. Uno de los objetivos esenciales de la herramienta es de ayudar a los operadores del sistema, proporcionando imágenes con características fácilmente identificables, las cuales, están relacionadas con el deterioro global de la calidad de la energía. El resultado es una interfaz amigable tridimensional. La eficacia de la herramienta se ilustra mediante diferentes escenarios que se recrearon con el sistema de prueba IEEE de 13-barras.**

***Palabras claves*— *E*valuación de la calidad de la potencia, mapas de calidad de la potencias, mediciones de calidad de la potencia, análisis tensorial.**

[1] M.Sc., Electrical Engineer, Universidad Industrial de Santander, Ph.D. in Engineering, Universidad Nacional de Colombia, Colombia. Associate Professor with the Department of Electrical, Electronic and Computer Engineering, Universidad Nacional de Colombia, Manizales Branch, Manizales–Colombia, e-mail: ajustarizf@unal.edu.co.

[2] Specialist, Electrical Engineering, Universidad Nacional de Colombia, Ph.D. in Engineering, Universidad de Buenos Aires, Argentina. Professor with the Department of Electrical, Electronic and Computer Engineering, Universidad Nacional de Colombia, Manizales Branch, Manizales–Colombia, e-mail: eacanopl@unal.edu.co.

[3] Electrical Engineering, Universidad de Buenos Aires, Argentina, M.Sc., and Ph.D. University of Sciences and Technologies of Lille, France, Ph.D. in Engineering, Universidad de Buenos Aires, Argentina. Professor with the Department of Electronic Engineering, Universidad de Buenos Aires, Buenos Aires – Argentina, e-mail: htacca@fi.uba.ar.

1. INTRODUCTION

Effective power system operation means that power system engineers and operators must analyse vast amounts of information. A key challenge in systems containing thousands of buses is to present this data in a form allowing a user to intuitively and quickly assess the state of the system (Santoso *et al*, 2000; Gu and Bollen, 2000).

This is particularly true when trying to analyse electrical network power quality. Therefore, constructing maps regarding power quality loss or deterioration due to steady-state and non-stationary events is of great importance for controlling, protecting and analysing power systems. Typically, efforts at drafting maps are focused on analysing the voltage signal. This is done by simulation programmes and electrical events using sophisticated measuring and monitoring the voltage (instantaneous values or RMS) at specific nodes of the particular system being studied. This information is analysed by systems' experts for detecting and classifying disturbances present in the voltage waveform (Gauoda *et al*., 2002; Wang *et al*., 2004; Duque *et al*., 2006; Cerqueira *et al*., 2006; Mosoum *et al*., 2010). The results are subsequently displayed by using in two- and three-dimensional visualisation techniques (Weber, and Overbye, 2000; Overbye *et al*., 2003; Overbye, and Weber, 2001; Klump and Weber, 2002; Sun and Overbye, 2004; Xu *et al*., 2006; Overbye *et al*., 2007; Evrenosoglu *et al*., 2007; Milano, 2009).

This form of presenting the state of an electrical system's variables to the network operator can be helpful when making decisions, but it can become a very tedious task which is difficult to interpret if many indicators must be analysed simultaneously. It should also be borne in mind that the bars may represent many power systems.

This paper describes a technique for three-dimensional visualisation and animation of the deterioration of power quality in electrical networks based on power tensor theory. The technique's objective is to provide electrical network images having easily identifiable characteristics by constructing graphical schemes or maps of power quality loss. The tool's effectiveness is illustrated via different scenarios which were created using the 13 bus distribution system reported by the Institute of Electrical and Electronics Engineers' (IEEE) subcommittee on distribution system

analysis (Distribution Planning Working Group Report, 2001).

2. THREE-DIMENSIONAL VISUALIZATION AND ANIMATION

a) Background Review

The importance of an intuitive and detailed visualisation of results produced by a disturbed power system has been discussed since late in the past century. Two-dimensional visualisations based on one-line diagrams have been relatively popular due to power system operators' familiarity with one-line diagrams and the importance of geographical information in power system operation and control.

Examples of this can be found in work where two-dimensional contour plot are proposed for visualising voltage levels in each power system bus (Weber, and Overbye, 2000; Overbye *et al*., 2003; Overbye, and Weber, 2001). Similarly, the contour plot technique has been further developed for visualising a variety of data such as power flows, marginal prices, available transfer capability, contingency analysis, etc (Klump and Weber, 2002; Sun and Overbye, 2004; Xu *et al*., 2006; Overbye *et al*., 2007). All these references focus on static data visualisation and are basically two-dimensional plots. By contrast with the two-dimensional visualisation techniques listed, three-dimensional visualisation and animation has also been proposed (Evrenosoglu *et al*., 2007; Milano, 2009).

b) Proposed Visualization Technique

The basic functioning of the proposed visualisation and animation tool is shows in Figure 1. A three-dimensional visualisation and animation tool needs two source files, one for topological data (Simulink) and another for numerical data (EMTP-ATP).

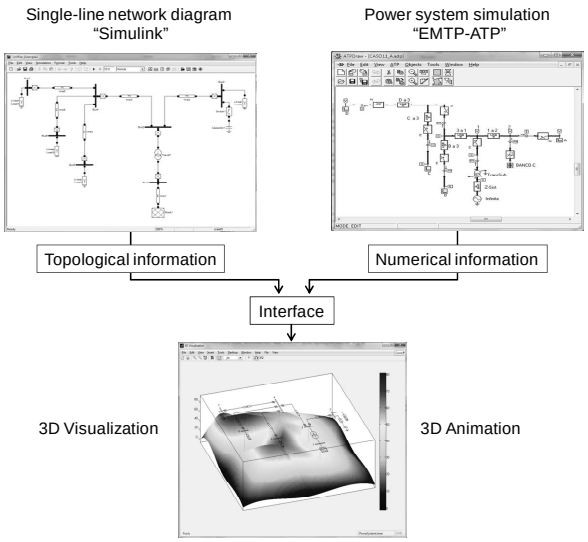

Figure 1. Basic functioning of the proposed visualisation and animation tool

The three-dimensional plots in this work have been obtained by computing the convex hull enveloping the values obtained from simulations onto a high-resolution three-dimensional surface. For example, if a power network's power quality deviator factor is considered than the number of available deviator factor values is equal to the number of connected meters, typically not being sufficiently high enough to adequately fill up the surface. To overcome this issue, a grid was created having a high number of points through polynomial interpolation. Next, the height of each point of the grid was determined by using Delaunay triangulation (Skiena, 1998). The resulting surface was finally coloured using a contour map and the one-line diagram of the network was superposed.

MATLAB was used to compute the Delaunay triangulation and plot results. The main functions used for displaying graphics schemes are polynomial interpolation (griddata.m), convex hull (convhull.m), Delaunay triangulation (delaunay.m) and contour maps (colormap.m).

3. POWER TENSOR THEORY

a) Instantaneous Power Tensor Definition

The proposed technique was based on the definition of an evolutionary expression of instantaneous power called *"instantaneous power tensor"* for geometrically interpreting electric phenomena behaviour, analogous to deformation studies in the mechanics of solids. Ustariz *et al*., using the tensor product, defined the instantaneous power tensor as follows (Ustariz *et al*., 2010A):

$$\wp_{ij} = u_i \otimes i_j \tag{1}$$

where, $\wp_{ij}$ was the instantaneous power tensor, u_i was the phase voltage tensor and i_j was the line current tensor. The instantaneous power tensor was expressed in an *n*-phase and *m*-wire system as:

$$\wp_{ij} = \begin{bmatrix} u_1 \\ u_2 \\ \vdots \\ u_n \end{bmatrix} \otimes \begin{bmatrix} i_1 \\ i_2 \\ \vdots \\ i_n \end{bmatrix} = \begin{bmatrix} u_1 i_1 & u_1 i_2 & \cdots & u_1 i_n \\ u_2 i_1 & u_2 i_2 & \cdots & u_2 i_n \\ \vdots & \vdots & \ddots & \vdots \\ u_n i_1 & u_n i_2 & \cdots & u_n i_n \end{bmatrix} \tag{2}$$

Here, the main diagonal terms ($u_i i_i$) referred to the instantaneous energy flow. Moreover, the differences between the transposed terms ($u_i i_j$-$u_j i_i$ with $i \neq j$) referred to the instantaneous energy exchange between phases *i* and j whose average was zero (Ustariz *et al*., 2010B). Therefore, $\wp_{ij}$ was a single expression which involved the two conventional components of instantaneous power (active and reactive).

b) Power Quality Deviation Factor

The measurement and evaluation of nonconformities in a disturbed power system could be quantified by defining a new overall power quality index called instantaneous power quality deviation indicator (IDI). It would be evaluated using the following expression:

$$IDI_{pq} = \left[\frac{\sum_{i=1}^{n} \sum_{j=1}^{n} \left(\wp_{ij} - {}^{ideal}\wp_{ij} \right)^2}{\sum_{i=1}^{n} \sum_{j=1}^{n} {}^{ideal}\wp_{ij}^2} \right]^{\frac{1}{2}} \quad (3)$$

where the term ${}^{ideal}\wp_{ij}$ would be defined as the ideal power tensor. Calculating an ideal power tensor involves defining an ideal electrical system as being a circuit consisting of a sinusoidal, balanced voltage source (ideal voltage tensor) feeding a resistive, balanced linear load (ideal current tensor).

Moreover, the root mean square of IDI_{pq} has been called the power quality deviation factor (DF) DF_{pq}, so that:

$$DF_{pq} = \left[\frac{1}{(t_2 - t_1)} \int_{t_1}^{t_2} IDI_{pq}^2 \, dt \right]^{\frac{1}{2}} \quad (4)$$

Here, the interval defined between t_1 and t_2 matched the temporal observation window's width. A 12-cycle window is recommended when working frequency is 60 Hz (IEC Std. 61000-4-30, 2003). In (4), zero indicated a null deviation regarding an ideal power system.

The notable features of definition (4) are the following:

- It provides quick assessment of power transfer quality deterioration from the ideal in terms of maximum power transfer;
- It is regardless of whether the disturbance arises from the load or the source; and
- It does not use controversial or misleading quantities such as traditional indexes' average, maximum or weighting values.

Additionally, the power quality deviator factor can have several useful applications:

- Sites having poor power quality could be easily ranked to determine priority for power quality improvements;
- It can be easy to represent by constructing graphical schemes or maps of power quality loss in large electrical networks; and
- System operators will have a single index which they can correlate with planning, protection or maintenance practice.

c) Comparison Criteria

Power quality deterioration assessment is traditionally based on individual indicators, such as total harmonic distortion (THD_X), unbalance factor (UF_X) and reactive power factor (PF_R) (Milanez and Emanuel, 2003; Emanuel, 2004; Sharon *et al*., 2008). The conventional definitions are:

- Total harmonic distortion of the voltage and current

$$THD_V = \frac{V_{eH}}{V_{e1}}; \qquad THD_I = \frac{I_{eH}}{I_{e1}} \quad (5)$$

- Unbalance factor of the voltage and current

$$UF_V = \left[\frac{V_{e1}^2 - {}^{+}V_1^2}{V_{e1}^2} \right]^{\frac{1}{2}}; \qquad UF_I = \left[\frac{I_{e1}^2 - {}^{+}I_1^2}{I_{e1}^2} \right]^{\frac{1}{2}} \quad (6)$$

- Reactive power factor

$$PF_R = \left[\frac{{}^{+}S_1^2 - {}^{+}P_1^2}{{}^{+}S_1^2} \right]^{\frac{1}{2}} \quad (7)$$

Expressions (5) to (7) were based on (IEEE Std-1459, 2000), where sub indexes 1 and *H* indicated fundamental and harmonic frequency components. Super indexes + referred to the direct sequence component; *S* and *P* referred to apparent and active power.

4. SIMULATIONS

Different scenarios have been created in this section, using IEEE 13-bus test feeder (see Figure 2) to illustrate the benefits of using proper visualisation methods in monitoring power quality in electrical networks based on power tensor theory.

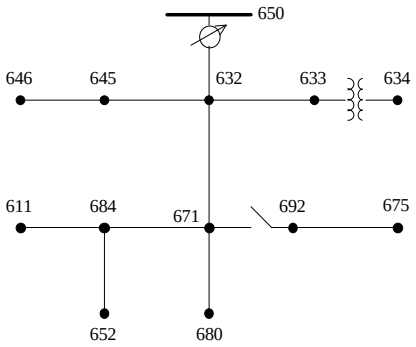

Figure. 2. IEEE 13-bus test feeder [17]

a) Scenario No. 1: (base case)

The IEEE-13-bus test feeder presents some very interesting characteristics, such as being short and relatively highly loaded for a 4.16 kV feeder, having one substation voltage regulator consisting of three single-phase units connected in wye, overhead and underground lines having a variety of phasing, shunt capacitor banks, in-line transformer, unbalanced spot and distributed loads.

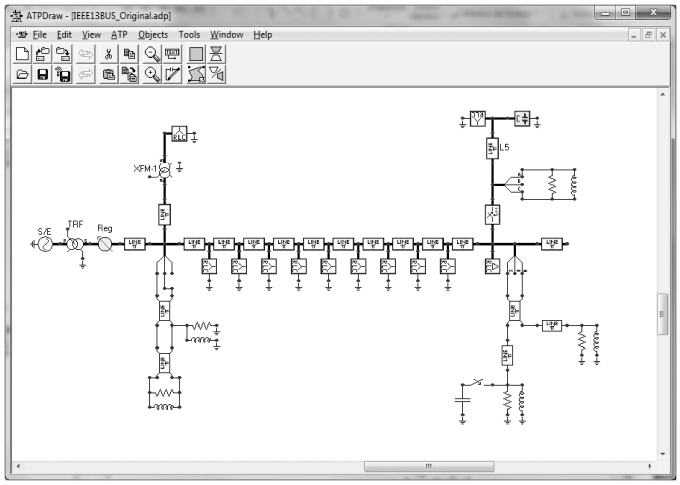

Figure 3. IEEE 13-bus test feeder implemented in "EMTP-ATP"

The IEEE 13-bus test feeder was implemented in EMTP-ATP (see Figure 3).

On the other hand, the IEEE 13-bus test feeder presented three types of steady-state disturbance: voltage imbalances, load unbalance and reactive power flows. These disturbances were measured and the results are summarised in Table I.

Table 1. Power Quality Index Measurement in Scenario1

	Individual indexes (%)					Overall index (%)
Node	THD_V	THD_I	UF_V	UF_I	PF_R	DF_{pq}
650	0.00	0.00	0.41	19.80	40.93	47.47
RG60	0.00	0.00	0.50	18.87	40.91	47.20
632	0.00	0.00	1.00	18.87	37.60	43.26
633	0.00	0.00	1.02	8.09	59.36	74.35
634	0.00	0.00	1.01	19.03	58.70	73.93
645	0.00	0.00	52.38	77.48	51.72	110.67
646	0.00	0.00	52.36	70.71	43.55	114.42
671	0.00	0.00	2.85	43.31	25.83	45.92
680	0.00	N/A	2.85	N/A	N/A	N/A
684	0.00	0.00	52.32	81.56	12.41	106.72
611	0.00	0.00	77.46	91.29	8.62	122.69
652	0.00	0.00	77.46	91.29	71.82	143.44
692	0.00	0.00	2.86	72.61	4.01	68.01
675	0.00	0.00	3.03	76.28	13.86	69.54

As expected, nodes 652 and 611 (single-phase sections) had the highest levels of quality loss (143.44% and 122.69% respectively) followed by nodes 646 and 645 (two-phasing sections: 114.42% and 110.67%, respectively). These nodes also had the highest UF_V, UF_I and PF_R indexes, except for the PF_R index in node 611, which was low by the shunt capacitor banks.

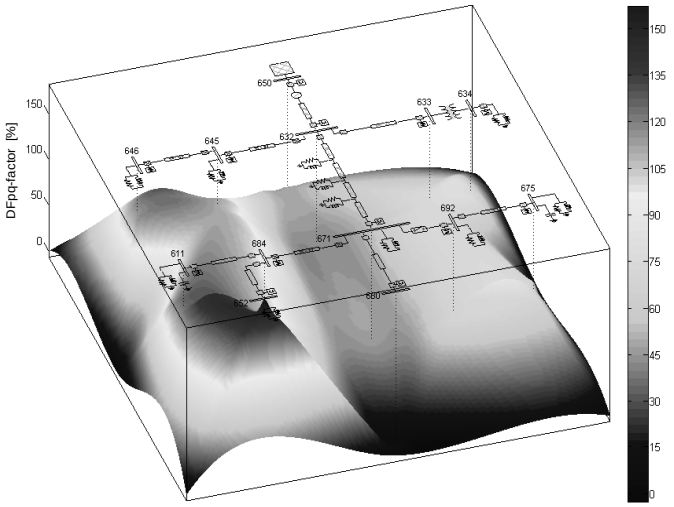

Figure 4. Map of quality loss and one-line diagram of the IEEE 13-bus test feeder for scenario 1

Figure 4 simultaneously shows a map of quality loss and a topological scheme. Here, the colour indicator shown on the right-hand side of the map presents the levels as a percentage of power quality deviation factors DF_{pq}. Dark blue represents non-deterioration of power quality while dark red means greater power quality deterioration.

b) Scenario No. 2: (harmonic distortion).

The linear load connected at node 634 was changed for a six-pulse adjustable-speed drive (ASD-6P) in this scenario. The main ASD-6P parameters were 480 V nominal line voltage, nominal 600 kVA rated three-phase power and 0.8 power factor.

The base case was modified to characterise a non-linear load connection in the IEEE 13-bus test feeder and construct a power quality loss map in steady state.

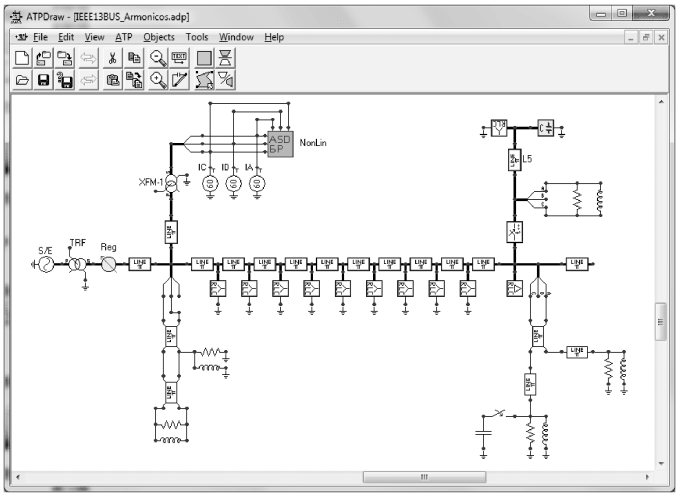

Figure 5. IEEE 13-bus test feeder modified for scenario 2

Figure 5 shows the modified IEEE 13-bus test feeder circuit which has been simulated in EMTP-ATP. This circuit shows the adjustable-speed drive model used.

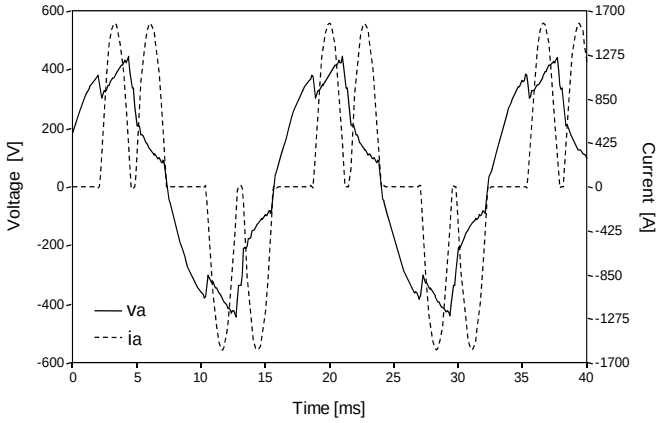

Figure 6. Voltage and current waveforms at ASD-6P input

Figure 6 shows voltage and current waveforms at the ASD-6P entrance (node 634). The remaining nodes in the modified test system had a noticeable influence on harmonic distortion propagation (Table 2).

From the results summarised in Table 2, as expected, nodes 634 and 633 became the next in importance in terms of quality deterioration. These nodes had a 45% increased loss of quality compared to the base case.

TABLE 2
POWER QUALITY INDEXES MEASUREMENT IN SCENARIO 1

	Individual indexes (%)					Overall index (%)
Node	THD_V	THD_I	UF_V	UF_I	PF_R	DF_{pq}
650	2.10	12.79	0.38	18.71	41.92	50.45
RG60	2.09	12.88	0.49	17.76	41.90	50.22
632	5.34	12.87	0.94	17.76	38.55	46.74
633	6.04	67.24	0.94	0.00	61.02	117.23
634	14.73	67.24	0.72	0.00	60.16	118.86
645	5.24	5.10	52.37	77.48	51.71	111.17
646	5.24	4.46	52.34	70.71	43.52	114.85
671	7.27	12.37	2.79	43.31	25.83	49.04
680	7.27	N/A	2.79	N/A	N/A	N/A
684	6.02	19.54	52.33	81.55	12.43	108.39
611	5.15	17.32	77.46	91.29	8.62	123.81
652	6.88	4.88	77.46	91.29	71.82	144.21
692	7.27	20.25	2.79	72.59	4.00	73.63
675	7.61	22.57	2.97	76.27	13.85	77.07

Figure 7 compares power quality loss maps and two-dimensional visualisation for the base case, as in the case of harmonic distortion.

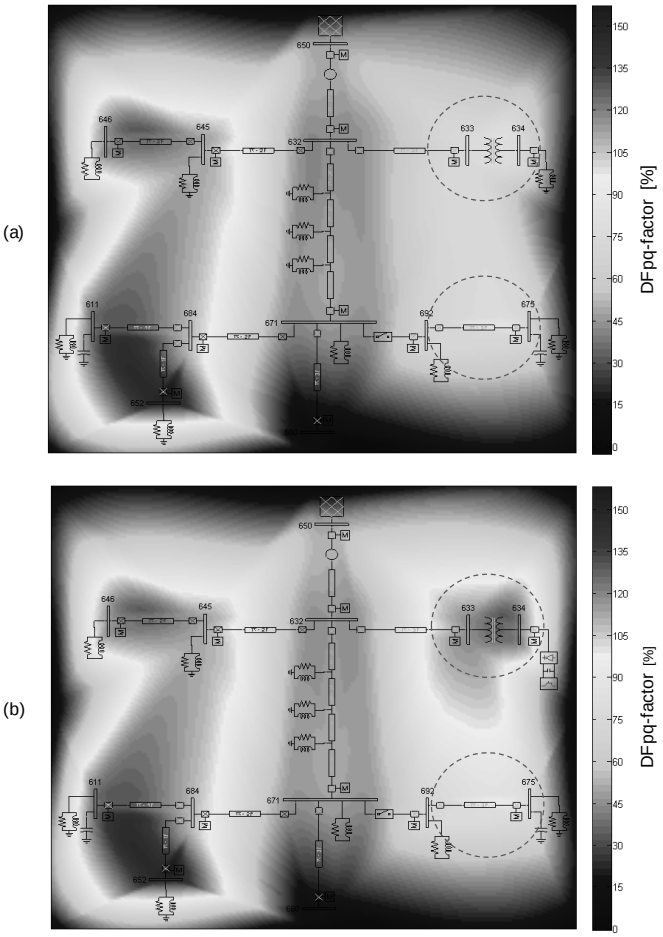

Figure 7. Two-dimensional quality loss maps: (a) scenario1 *base case* and (b) scenario 2 *harmonic distortion*

Two areas of the map are outlined in dotted lines in Figure 7(b), showing increased DF_{pq}-factor values for scenario 2. The first and most notable case occurred in the distribution transformer located between nodes 633 and 634. The second was less noticeable and was given in the section consisting of nodes 692 and 675. These variations were immediately obvious by observing the colour change compared to the same location in Figure 7(a).

c) Scenario No. 3: (propagation of a transient disturbance).

A single-phase fault (in phase-b) was caused in the line connecting nodes 632 and 671. The fault occurred at t=1.1s, lasting 70ms and fault impedance was 0.5 Ω.

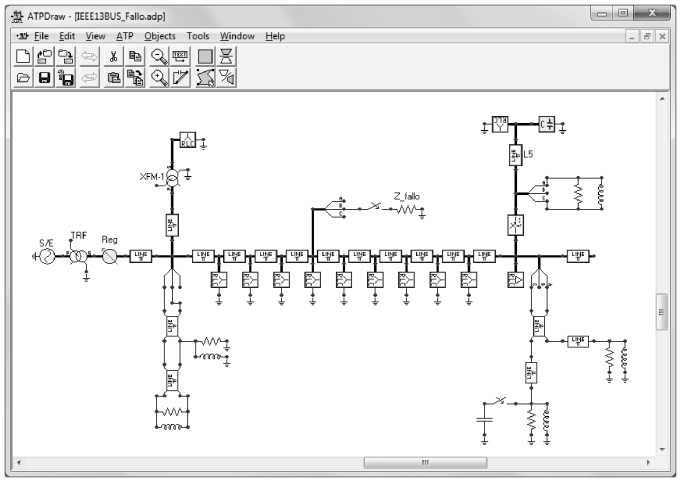

Figure 8. IEEE 13-bus test feeder modified for scenario 3

Figure 8 shows a fault model developed from a switch connected to phase-b in series with ground resistance.

The records for voltage and current waveforms upstream of the fault are shown in Figure 9.

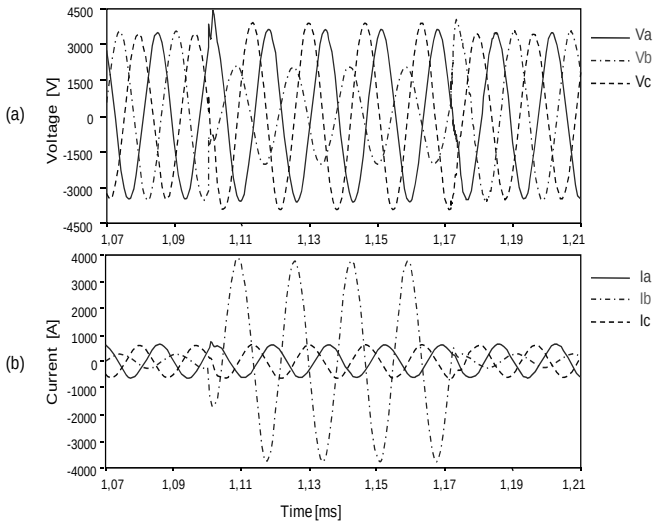

Figure 9. Waveforms upstream of the fault: (a) voltage and (b) current

As can be seen in Figure 9(b), phase-b current became increased upstream of the fault because of with little resistance being offered by the fault impedance. Moreover, the single-phase fault also occurred in system sag and voltage swell nodes, as shown in Figure 9(a). It can be seen that phase-b voltage became decreased by almost 50% while phase-a and phase-c voltage became slightly increased.

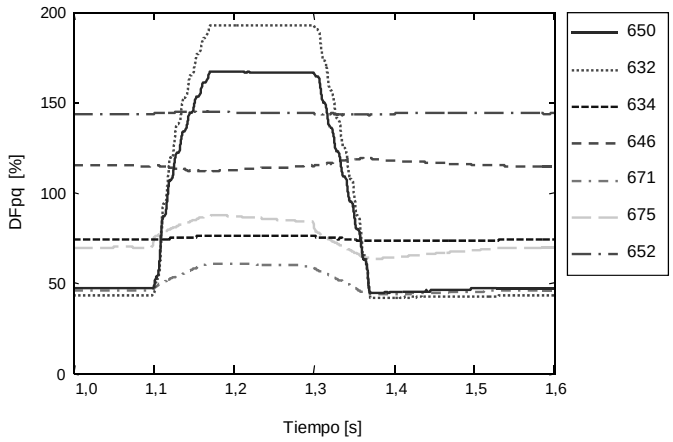

Figure 10. *DFpq-factor* measured at different nodes in scenario 3

Figure 10 shows the DF_{pq}*-factor* detected as a non-stationary event in the system's different nodes. Figure 10 clearly shows that nodes 650 and 632 had the highest levels of quality loss during the single-phase fault. Quality loss compared to the values before the fault changed very little in the rest of the nodes; no changes were seen in nodes 634 and 652.

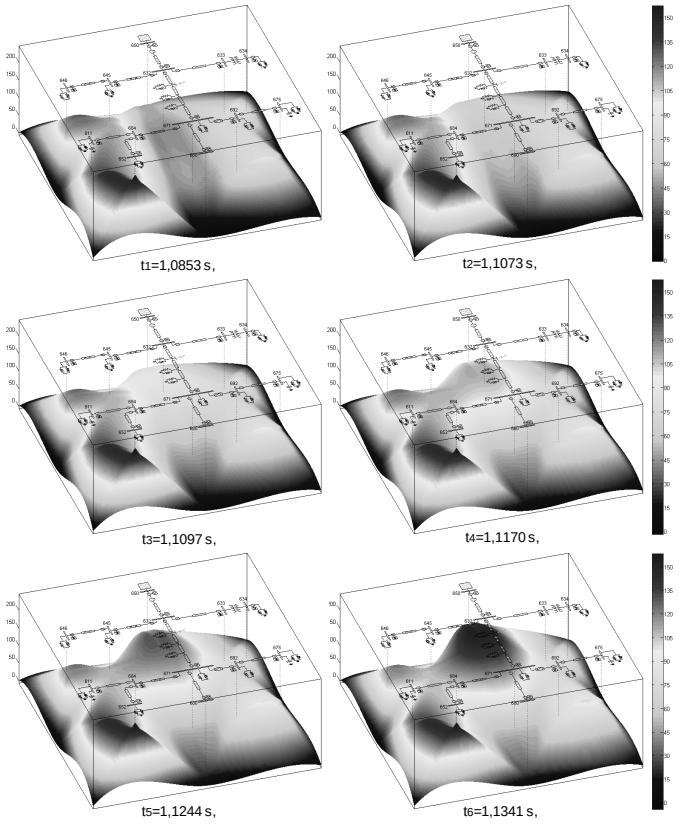

Figure 1. Frames from the three-dimensional animation of the quality loss map in scenario 3

On the other hand, using three-dimensional animation, one can intuitively show how the whole system was affected by quality loss during the single-phase fault. Figure 11 gives six snapshots showing the propagation of a transient disturbance for the IEEE 13-bus test feeder. Unfortunately, the snapshots did not fully illustrate the propagation of a transient

disturbance as well as the three-dimensional animation did; animation clearly showed how quality loss was propagated from one zone to another of the particular system.

5. CONCLUSIONS

This paper has described a software package developed as a system operator aid. The tool was based on a technique for assessing power quality deterioration in electrical networks, based on power tensor theory. It has shown a user-friendly interface allowing a user to construct a system diagram for a new power system or edit an existing one to make desired modifications.

Three-dimensional animation and colour contouring techniques have been used for visualising the integral evaluation of power transfer quality deterioration in power systems.

The examples of different cases led to verifying the proposed indicator's applicability when measuring power transfer quality deterioration.

Future work will concentrate on improving the three-dimensional visualisation technique. A promising development would be the inclusion of new technology, such as involving a geographical information system when constructing graphical schemes or maps.

6. ACKNOWLEDGEMENT

This work has been partly supported by the Universidad Nacional de Colombia, Manizales

7. REFERENCES

Cerqueira, A.S., Duque, C.A., Ribeiro, M.V., Trindade, R.M., Digital system for detection and classification of power quality disturbances, IEEE Latin America Transactions, Vol. 4, No. 5, Sep. 2006, pp. 345–352.

Duque, C.A., Ribeiro, M.V., Ramos, F.R., Szczupak, J., Power quality event detection based on the principle of divide to conquer and innovation concept, IEEE Trans. Power Del., Vol. 20, No. 4, Oct., 2005, pp.2361–2369.

Emanuel, A.E., Summary of IEEE standard 1459: definitions for the measurement of electric power quantities under sinusoidal, nonsinusoidal, balanced, or unbalanced conditions, IEEE Trans. Ind. Appl., Vol. 40, No 3,May/Jun. 2004, pp. 869–876.

Evrenosoglu, C.Y., Abur, A., Akleman, E., Three dimensional visualization and animation of travelling waves in power systems, Electric Power System Research, Vol. 77, No. 7, May, 2007, pp. 876–883.

Gaouda A.M., Kanoun S.H., Salama M.M.A., Chikhani A.Y., Wavelet-based signal processing for disturbance classification and measurement, IEE Proceedings - Generation, Transmission and Distribution, Vol. 149, No. 3, May, 2002, pp. 310–318.

Gu, Y., Bollen, M.H.J. , Time-frequency and time-scale domain analysis of voltage disturbances, IEEE Trans. Power Del., Vol. 15, No. 4, Oct., 2000, pp. 1279–1284.

IEC, Power quality measurements methods, Testing and Measurement Techniques, IEC Std. 61000-4-30.

IEEE Distribution Planning Working Group Report, Radial distribution test feeders, IEEE Power Engineering Society Winter Meeting, Columbus, Ohio, USA, Jan 28-Feb. 1, 2001, pp. 908–912.

IEEE Std. 1459, IEEE Trial-Use Standard Definitions for the Measurement of Electric Power Quantities under Sinusoidal, Nonsinusoidal, Balanced, or Unbalanced Conditions, Jan. 2000.

Klump, R.P., Weber, J.D., Real-time data retrieval and new visualization techniques for the energy industry, 35th Hawaii International Conference on System Sciences, Big Island, Hawaii, Jan. 7-10, 2002, pp. 712–717.

Masoum, M.A.S., Jamali, S., Ghaffarzadeh, N., Detection and classification of power quality disturbances using discrete wavelet transform and wavelet networks, IET Science Measurement & Technology, Vol. 4, No.4, Jul., 2010, pp. 193–205.

Milanez, D.L., Emanuel, A.E., The instantaneous-space-phasor a powerful diagnosis tool, IEEE Trans. Instrum. Meas., Vol. 52, No. 1, Feb 2003, pp. 143–148.

Milano F., Three-dimensional visualization and animation for power systems analysis, Electric Power Systems Research, vol. 79, no. 12, pp. 1638–1647, Dec. 2009.

Overbye, T.J., Rantanen, E.M., Judd, S., Electric power control center visualization using geographic data views, Symposium Bulk Power System Dynamics and Control – VII. Revitalizing Operational Reliability, Charleston, SC, USA, Aug. 19–24, 2007, pp. 1–8.

Overbye, T.J., Weber, J.D., Visualizing the electric grid, IEEE Spectrum, Vol. 38, No. 2, Feb., 2001, pp. 52–58.

Overbye, T.J., Wiegmann, D.A., Rich, A.M., Sun, Y., Human factors aspects of power system voltage contour visualizations, IEEE Trans. Power Syst., Vol. 18, No. 1, Feb., 2003, pp. 76–82.

S.S. Skiena, The algorithm design manual, Springer-Verlag, New York, 1998.

Sansoto, S., Grady, M.W., Powers, E.J., Lamoree, J., Bhatt, S., Characterization of distribution power quality events with Fourier and wavelet transforms, IEEE Trans. Power Del., Vol. 15, No. 1, Jan., 2000, pp. 247–254.

Sharon, D., Montaño, J., Lopez, A., Castilla, M., Borrás D., Gutierrez, J., Power quality factor for networks supplying unbalanced nonlinear loads, IEEE Trans. Instrum. Meas., Vol. 57, No. 6, Jun. 2008, pp. 523–527.

Sun, Y., Overbye, T.J., Visualizations for power system contingency analysis data, IEEE Trans. Power Syst., Vol. 19, No. 4, Nov., 2004, pp. 1859–1866.

Ustariz, A.J., Cano, E.A., Tacca, H.E., Instantaneous power tensor theory: improvement and assessment of the electric power quality, 14th International Conference on Harmonics and Quality of Power, ICHQP'2010, Bergamo-Italy, Sep. 2010, pp. 1–6.

Ustariz, A.J., Cano, E.A., Tacca, H.E., Tensor analysis of the instantaneous power in electrical networks, Electric Power Systems Research, Vol. 80, No 7, Jul. 2010, pp.788–798.

Wang, M., Rowe, G.I., Mamishev, A.V., Classification of power quality events using optimal time-frequency representations-Part 2: application, IEEE Trans. Power Del., Vol. 19, No. 3, Jul., 2004, pp. 1496–1503.

Weber, J.D., Overbye, T.J., Voltage contours for power system visualization, IEEE Trans. Power Syst., Vol. 15, No. 1, Feb., 2000, pp. 404–409.

Xu B., Yuksel C., Abur A., Akleman E., 3D visualization of power system state estimation, IEEE Mediterranean Electrotechnical Conference, Benalmádena, Spain, May 16–19, 2006, pp. 943–947.